Modeling of Automotive HVAC Systems Using Long Short-Term Memory Networks

Peter Engel
TU Clausthal
Institute for Software and Systems Engineering,
Clausthal, Germany
e-mail: peter.engel@tu-clausthal.de

Sebastian Meise
TLK-Thermo GmbH,
Braunschweig, Germany
e-mail: s.meise@tlk-thermo.de

Andreas Rausch
TU Clausthal
Institute for Software and Systems Engineering,
Clausthal, Germany
e-mail: arau@tu-clausthal.de

Wilhelm Tegethoff
TLK-Thermo GmbH,
Braunschweig, Germany
e-mail: w.tegethoff@tlk-thermo.de

***Abstract*— Adaptive and fast-calculating HVAC and climate models are gaining increasing importance in the automotive development process. Physically motivated thermal models achieve high quality results, but have a disadvantage in terms of their computing speed due to their complexity. One possible approach for the fast and precise simulation of thermal systems is deep learning with artificial neural networks. This paper aims to determine the extent to which neural LSTM are suitable for modeling the complex dynamic behavior of vehicle air conditioning. For this purpose, a physical reference model of a passenger car air conditioning system including a vehicle cabin is set up in the simulation environment Dymola with the component library TIL Suite. Furthermore, a model structure of a LSTM -based deep neural network to map the dynamic thermal behavior correctly is proposed. For the purpose of training the ANN, the overall system has been broken down into subsystems. The subsystems are individually trained open-loop and then linked to form a closed-loop overall model. For evaluation purposes, models with the same model structure but based on feed forward network (FFN) architectures are implemented, trained and tested.**

Keywords - BEV; Applied Machine Learning; HVAC; LSTM; ANN;

I. INTRODUCTION

In the automotive development process, simulations of the vehicle climate are required in order to test components, assemblies, system concepts and control variants in a cost-effective and time-efficient manner. Furthermore, simulations of the vehicle's climatization systems are currently gaining more and more of a focus on research, as they are used within Model-Predictive Controllers (MPC) to optimize HVAC control.

Previous work has shown that physical modeling shows good results and provides a good picture of real thermodynamic processes. A number of studies have focused on a detailed physical modeling of the cabin climatization for simulation purposes [1]-[14]. In addition to the vehicle interior temperature, energy consumption, air humidity and, in some cases, air quality and thermal comfort are also calculated in the form of a Predicted Mean Vote (PMV). With the modeling methods described here, it was possible to achieve high prediction accuracy in the sense of the accordance of measurement and simulation results. However, these models have a significant disadvantage of the modeling effort and the high runtime and are therefore not suitable for use in a model predictive controller. A compromise between run-time and prediction accuracy with relatively low modeling effort is provided by adaptive learning methods with modeling of the controlled system by Artificial Neural Networks (ANN). Previous work on simulating the cabin climate with ANN showed promising results for short forecast horizons. However, for longer forecasting horizons and at large operating range, the known works are only limitedly suitable for simulation in the vehicle development process or in use within an MPC. One reason for this is the error accumulation due to the multiple consecutive one-step-ahead predictions. The output of each prediction step along the prediction time window is used as the input for the following one. As a result, the error also propagates and resonates, resulting in high inaccuracies.

An alternative architecture of recurrent neural networks, which is particularly suitable for the prediction of time series, has been introduced with Long Short-Term Memory (LSTM) networks [15]. With the use of LSTM in their products, the major technology companies Apple, Alphabet and Microsoft have achieved great success in recent years. Based on this network structure, a deep neural network for the simulation of the cabin climate will be presented in this paper.

The modeling of physical systems using machine learning methods is subject to two major challenges. On the one hand, the right architecture, which is suitable for mapping the system dynamics well, must be found. The other problem consists in the quality of the learning data as the essential basis of all learning methods. The values of physical quantities obtained by measurements of physical processes are subject to deviations due to measurement uncertainties and measurement deviations. Since the quality of learning systems is limited by the quality of the learning data, preprocessing of the signals, e.g., by smoothing and filtering, is required. Since this work examines the suitability of the architecture for mapping the system dynamics, the training is based on learning data generated by a conventional system model. For this purpose, a complex detailed reference system model was created in a first step. Based on this ref-

 ISBN: 978-1-61208-706-1

erence system model, the quality of the examined learning methods was evaluated.

The following Section II describes the state of the art in terms of physical thermal modeling and modeling with ANN. In Section III the reference system model is presented. Subsequently in Section IV, the structure of the LSTM-based deep neural network is explained in more detail. Finally in Section V, simulation results of the comparison of NARX-based networks and LSTM-based networks are presented and discussed.

II. MODELING OF THERMAL SYSTEMS

A. Physical Thermal Modelling

The simulation of thermal models is an established element of the vehicle development chain. One reason is that development times are greatly reduced, since component tests can take place virtually without having to set up or modify a new test bench. The requirements on the models are not only a realistic representation of the real component but also the speed at which the model can be simulated. This requirement is particularly important for models that are used on real-time systems. Furthermore, the simulation time has a great influence on the duration of the development cycles and thus has a direct effect on the costs, which underlines the importance of this requirement once again. The demands posed to the model are matched by the challenges of modelling. These are among others:

- Realistic mapping of system and component complexity
- Transfer of the characteristics of individual components by means of parameterization
- Implementation of the physical behavior of individual components
- Checking the thermal behavior of circulation systems

One way to generate fast and realistic thermal models of components and systems is to use physical models. These use thermodynamic relationships to realistically model the interaction of a component with its environment. The advantage of the physical approach lies in the inherent quality of the representation of reality, provided that the laws can be fully captured and implemented. However, since even a seemingly simple component, e.g., the refrigerant pipe of an air conditioning system already spans a complex network of thermal dependencies. This makes physical modelling of thermal systems very demanding and therefore time-consuming. It can take several weeks until the modelling of a car air conditioning system has been modeled and validated. The more complex a model becomes, the more time it can take to simulate it. Here, the quality of the simulation result competes with the simulation speed.

1) Model exchange using FMU

A further argument for the model-based component development is the possibility of parallel work of different departments on a component by means of model exchange. This can be done, for example, by transferring a Functional Mock-up Unit (FMU) [16]. The creator of the model exports the model from his modeling software into the standardized FMU format. This creates a container file which contains all equation systems of the original model in the form of a DLL and thus makes them generally usable. Beside the DLL there is also an XML, which contains the interface description. With the FMU export, it is also possible to integrate the required licenses and thus make the simulation of the integrated model possible in the first place. In order to restrict the use of the license, it is limited to the simulation of the FMU. The user of the FMU can now integrate the original model (e.g. Modelica code) in the format of an FMU into his own software environment (e.g. Matlab or MS Excel) and simulate it.

B. Modeling of Themal Systems with ANN

In various previous works, the modeling of thermal systems with neural networks was investigated. The majority of the work is focused on the simulation of building HVAC systems. Thus, e.g. in [17] and [18], nonlinear autoregressive networks with exogenous inputs (NARX) are used to predict the indoor temperature and humidity in rooms. The networks are essentially Feed Forward networks, usually multilayer perceptrons (MLP), with the outputs being fed back. In addition to the current independent (exogenous) inputs and the previous outputs, time-delayed values of these variables are also used as input. Figure 1 shows the common used NARX architecture.

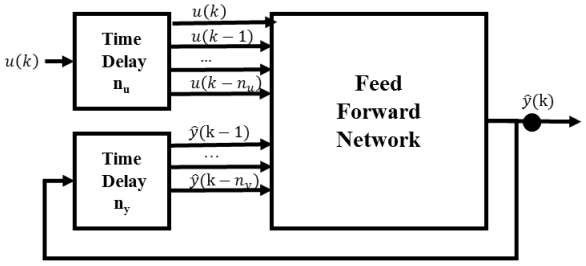

Figure 1 NARX Architecture

The training of the network is accomplished, without feedback, in a serial structure. Here, the true outputs $y(k-1, k-2, \ldots, k-n_y)$ are used instead of the predicted output $\hat{y}(k-1, k-2, \ldots, k-n_y)$. This has the advantage on the one hand that the exact inputs of the network are used. And on the other hand, a static backpropagation method such as the Levenberg Marquardt algorithm can be used as a learning method.

Based on this principle, several papers dealing with the modeling of building HVAC systems have been published. For example, in [19], multiple autoregressive RBF-ANNs are used to predict the PMV. The forecast result is used here within an MPC to reduce energy consumption while achiev-

ing maximizing thermal comfort. In [20], a series of recurrent models is used to predict humidity and indoor temperature in buildings. [21] also describes the use of a neural network to model a building HVAC system. This model is used as part of an intelligent energy management system in combination with a genetic algorithm to optimize the cooling energy requirement. The model consists of several submodels for the different components of the HVAC system, which are constructed as multi-layer perceptron (MLP) in feed forward structure with a hidden layer of 20 neurons, one bias and one hyperbolic activation function. The models predict the resulting exhaust temperature, fan pressure and compressor output. The model has a resolution of 1 minute. The mean average error MAE tested was 0.52K for the temperature model and 0.58 KW for the energy consumption.

The modeling of vehicle HVAC systems by neural networks was discussed in detail in [21]-[23]. In [22] and [23], the modeling of an experimental automotive air conditioning system with a recurrent, time-delayed neural network is described. The model is again used within a model predictive control to optimize the refrigeration cycle, in particular a variable speed compressor. The network has a hidden layer with 5 neurons and a time delay of 5 samples for the input and 3 samples for the feedback output. The data sampling rate was 8 seconds. The training was done on- and offline with a Levenberg-Marquardt algorithm. Tests using one-step-ahead and 10-steps-ahead prediction were performed. Here, it was determined that the feedback caused a fault accumulation, which is why an error resetting was performed after the 10 steps.

An artificial neural network architecture alternative to NARX exists with LSTM networks. In this case, as with all recurrent structures, not individual data points but entire sequences of the data are processed further. The feedback takes place here on the level of individual cells. Unlike traditional RNNs, the problems of exploding or vanishing gradients in training LSTMs have a much smaller impact. While the base element in feed forward networks is a single neuron with associated weights and an activation function, individual LSTM-units respectively LSTM-blocks are the base elements in LSTM networks. The common architecture of an LSTM-unit consists of one cell and three gates. The cell represents the memory of the unit. During each calculation step, the output of the LSTM-unit h_t (hidden state) and the state of the cell c_t are calculated.

The output of the LSTM-unit is calculated from the state of the cell and the output of the output gates. The cell state is calculated from the previous value of the cell state and the outputs of the input gates and the forget gate. In each of the three gates, as in a neuron in a feed forward network, each output is calculated from a weighted sum and an activation function. Through the training, the weights of the gates are adjusted and thus learned to what extent information from previous steps are stored or removed. The detailed description of the method can be found in [15].

Based on this basic architecture, Section IV proposes a deep neural network for mapping the thermal behavior of vehicle interior climate control. This model is trained on the data of a reference model, which is explained in more detail in the following chapter.

III. PHYSICAL REFERENCE MODELL

A. Model Design

In the simulation environment Dymola, the model of a mobile refrigeration system and a car cabin was created using the modeling language Modelica, the ModelicaStandardLibrary and the model library TIL Suite [24]. The air conditioning system used as a reference system comes from a Volkswagen e-Golf, which was available as a measuring vehicle for several months. The data collected was used to create a model of the vapor compression cycle, the climate control system and the cabin. The coarse structure of the refrigeration system model is shown in Figure 2.

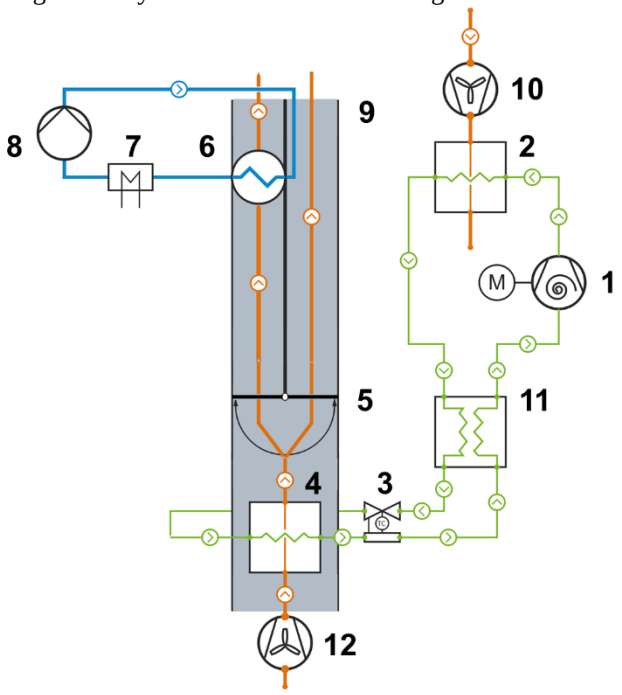

Figure 2 Refrigeration cycle with a scroll compressor (1), a high-pressure-side external air-refrigerant heat exchanger as condenser (2) with a fan (10), an internal heat exchanger (11), an expansion element (3) and the inner heat exchanger as evaporator (4). In the air duct (9) there is a temperature flap (5) which divides the air flow coming from the fan (12) and, depending on the operating point, directs it via the heat exchanger in the water-glycol cycle (6) of the heating circuit. The medium is heated by a high-voltage PTC (7) and circulated by a pump (8).

B. Refrigeration System Model

Compressor: The refrigeration cycle is operated with the refrigerant R-1234yf and consists of a scroll compressor taken from the TIL standard library. By adjusting its displacement volume and efficiencies, it was adapted to the compressor from the real refrigeration cycle. Internal pres-

sure and friction losses as well as heat dissipation to the environment are also mapped by the model.

Heat exchangers: The refrigerant-side heat exchangers used are from the TIL AddOn Automotive [25] and have been adapted to the dimensions of the e-Golf heat exchangers. The heat exchangers can be adapted to the real component via several parameters for geometry (see Figure 3), as well as heat transfer and pressure loss relationships.

Following the recommendation of Rohsenow et al. [26], the correlation of Gnielinski [27] for Reynolds numbers less than 2300 and the correlation of Dittus/Boelter [28] for Reynolds numbers greater than 104 was used for the calculation of the refrigerant-side heat transfer coefficient for the case of turbulent flow. For the phase change in the condenser, the correlation of Shah [29] was used. The air-side forced heat transfer was determined with the correlation established by Haaf [30]. For the refrigerant-side pressure loss during the phase change, the McAdams approach [31] in combination with the Swamee/Jain formulation [32] was used for Reynolds numbers greater than 2300 on the basis of the homogeneous calculation model. The implementation of the airside pressure loss was neglected.

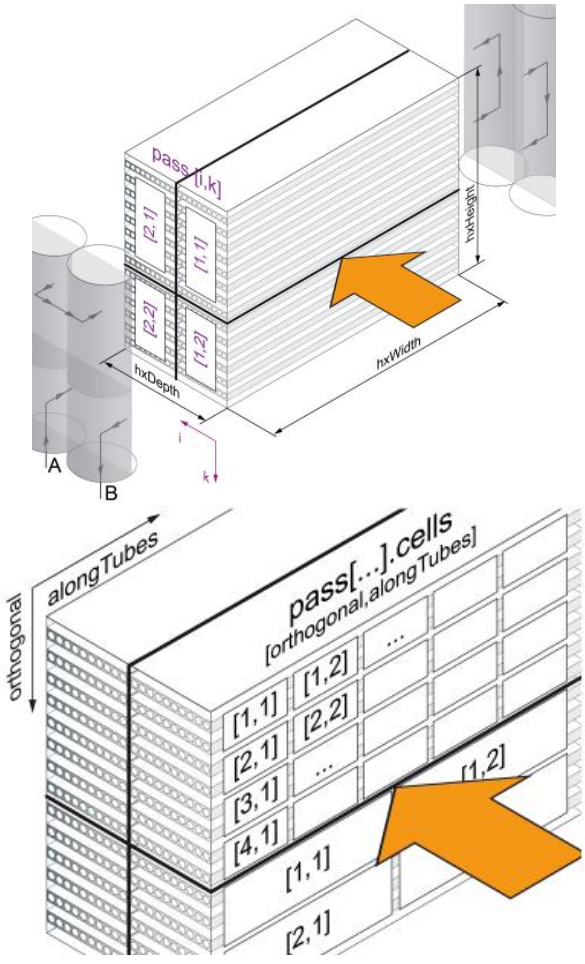

Figure 3 Modelling of heat exchangers with the TIL AddOn Automotive. The geometry of the heat exchangers can be completely adapted to that of the original component (upper illustration). Furthermore, the heat exchanger can be divided into cells (lower illustration). This allows a three-dimensional analysis of the heat exchanger [25].

High-voltage PTC: The high-voltage PTC was implemented via a heat source that transfers a loss-free heat flow to a tube model. The coolant, which absorbs the heat flow of the PTC with a defined heat transfer coefficient, is conducted through this tube model.

Expansion Valve: The expansion element is a thermostatic expansion valve. The opening behavior of the valve was implemented in the model based on manufacturer data. The nominal high- and low-pressure values are 9.7 bar at 235 cm³/h and 3.7 bar at 160 cm³/h. The maximum operating point is 7 bar at 35°C.

Fans: The fans are implemented as simple models which convey a defined air volume flow. Since no reliable air-side measurement data was available, no air-side pressure losses were integrated.

C. Vehicle Cabin System Model

The interior model comes from the TIL AddOn Cabin [33] and is based on an ideally mixed zero-dimensional air volume (moist air), which is thermally coupled to the passengers and surrounding surfaces (walls, windows, floor, ceiling, dashboard, seats) and these in turn to the environment (see Figure 4). The surface elements were implemented using parameters for geometry, material properties and heat transfer relationships.

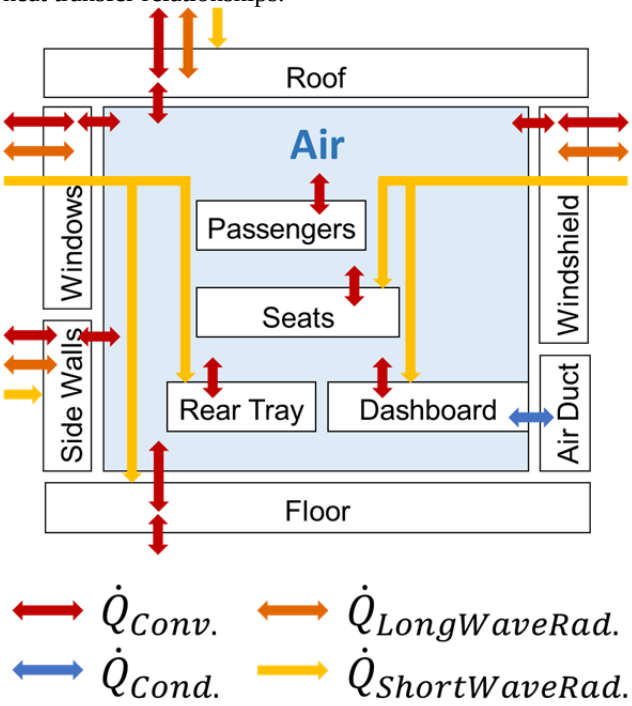

Figure 4 Structure of the cabin model with thermal connections of the individual components. In order to maintain the clarity, the representation of the long-wave radiation exchange of all components among each other, which is determined by view factors, was omitted

 ISBN: 978-1-61208-706-1

The air duct was modelled with a tube model available in TIL and thermally coupled to the underside of the dashboard. The passenger was integrated into the cabin model as heat and moisture source.

D. Comparison of Simulation and Measurement

The model was calibrated with several measurement runs and adapted via a fitting process. Since the climate control system uses the interior temperature as the central reference value, this quantity in particular is an important quality criterion for the model. Figure 5 shows a comparison of an exemplary simulation of a heating case. It can be seen that the interior model is not able to reproduce small temperature changes of the sensor. This is due to the ideal mixing of the air volume based on the zero-dimensional approach. However, the average heating behavior of the interior is very well represented. This results in a deviation of the interior temperature determined by the model of a maximum of 4.8K during the heat-up phase and a maximum of 0.9K in control mode over all evaluated test runs.

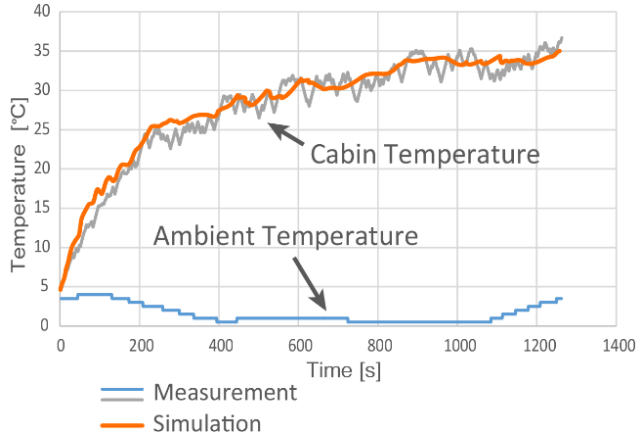

Figure 5 Comparison of measurement and simulation data of a test drive at an outside temperature between 0°C and 5°C.

The climate control system of the model was based on a typical control unit for electric vehicles. The model can dynamically map the following operating states:

- Heating
- Cooling
- Dehumidification
- Re-heating
- Ventilation

For the work presented here, the focus was on the operating states of heating and dehumidification. The resulting model of HVAC system and cabin consists of 9947 dependent parameters, 468 continuous time states, 199 linear equation systems with at most 2nd order, 32 non-linear equation systems with at most 1st order. The average CPU time is 240 seconds for 1000 simulated seconds. It was exported as FMU to perform the further process of ANN learning in Matlab and Python.

IV. MODELING OF THE CLIMATE SYSTEM WITH ANN

A. Model structure

The overall model consists of 6 linked submodels. Each submodel consists of an individually trained network. The submodels were each selected according to the sensors present in the vehicle, so that the signal trajectories of the inputs and outputs can be used as training data. The inputs of each subnet consist of feedback outputs of its own and other subnets, the direct outputs of other subnets and external inputs. Figure 6 shows simplified the overall model structure.

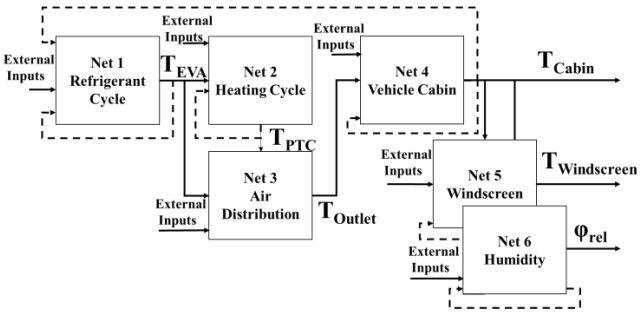

Figure 6 Model structure of the ANN-model

In the first subnet named the refrigerant cycle, the air temperature after the evaporator is predicted. For this purpose, the trajectories of the inside temperature, the outside temperature, the relative humidity inside and outside, the recirculation flap position, the fan power and the compressor power are used as inputs, each in the form of a sequence.

The second network represents the heating circuit. The trajectories of the electrical power of the PTC element, the air temperature after evaporator, the past air temperature after the heat exchanger, the temperature flap position and the fan power serve as input to predict the current air temperature behind the heat exchanger of the heating circuit. The predicted output values of the first two nets are used together with the position of the temperature flap and the blower output as input for the third network, the air distribution, to predict the outlet temperature at the vents to the cabin interior.

In the fourth network, the new internal temperature is calculated from a number of external inputs, such as outside temperature, direct and diffuse solar radiation power, vehicle speed, fan power, passenger number and past internal temperature and outlet temperature. From this, the new windscreen temperature and the resulting new relative humidity are predicted in the last two networks.

B. Network Architecture / Parameterization

1) NARX

The NARX networks were designed as in the work described in Section II.B, each with a hidden layer with different numbers of neurons (5, 10 and 20). The input signals of the networks were prepared according to the different tested delays of 3 and 6 delay steps. For preprocessing of the signals, the training data of the inputs and outputs was normal-

ized by their mean value and their standard deviation. To generate the training data, 11 simulation runs were carried out with simulated journey duration of approx. 1 hour each. Here, a total of 40810 data samples were generated with a sampling rate of one second. The training data was subdivided as usual into learning, test and validation sets. As a learning function, the Levenberg-Marquardt algorithm was chosen with mean square error (MSE) as performance indicator. The training was carried out for each submodel with the different architectures and tested on 3 further unseen simulation runs with 10586 data samples. A maximum number of 200 learning epochs was defined as abort criterion for the learning processes. However, this never occurred because of the rapid convergence of the learning function. The RMSE was selected as benchmark for the evaluation of the test result.

2) LSTM

The LSTM networks were designed with a sequence input layer, a LSTM layer with different number of LSTM-units (5, 10 and 20), a fully connected layer and an output regression layer. Sequence lengths of 3 and 6 samples were examined. The input data was prepared as described above. For network training the adaptive moment estimation optimizer (ADAM), stochastic gradient descent optimizer (SGD) und the root mean square propagation optimizer (RMSProp) were tested. Here, too, a maximum number of 200 learning epochs was defined as the abort criterion of the learning processes. All learning methods showed a significantly weaker convergence compared to the NARX training procedures, so that the learning processes were always aborted due to the reached maximum number of learning periods. The SGD method proved to be the most efficient learning method. A mini batch size of 50 data samples per iteration was chosen. The test procedure was carried out as described above.

3) Combined Overall Model

To simulate the holistic system model, the individual subnetworks were linked according to the model structure shown in Section III.4. Here, the inputs were replaced by the direct and feedback outputs of the coupled individual subnets. The overall system was then tested by the three additional generated unseen test drive simulations.

V. TEST OF THE SUBMODELS AND THE COMBINED OVERALL MODEL

In accordance with the test methodology described in Chapter IV, the individual subnets were first tested using unseen described test data. In the first test series, the individual subnets were tested open loop with perfect input. This corresponds to the quality of a one-step-ahead prediction. Tables I and II show the results with the RMSE over all 3 test drives. It should be noted that the subnets 1-5 each have a temperature in K as a prediction variable and the subnet 6 a relative humidity in %.

The predictions of the NARX networks have significantly lower error rates compared to the predictions with LSTM networks. The error rates of the LSTM networks decrease with increasing network architecture complexity.

TABLE I. *RESULTS OF THE NARX OPENLOOP SUBNET TEST*

Number of Hidden Layer Neurons	Number of Delays	RMSE Net 1	RMSE Net 2	RMSE Net 3	RMSE Net 4	RMSE Net 5	RMSE Net 6
5	3	0,0031	0,0035	0,0096	0,0004	0,0001	0,0111
5	6	0,0037	0,0031	0,0024	0,0013	0,0005	0,0052
10	3	0,0036	0,0045	0,0046	0,0017	0,0008	0,0167
10	6	0,0136	0,0031	0,0076	0,0004	0,0001	0,0059
20	3	0,004	0,0029	0,0019	0,0003	0,0003	0,0061
20	6	0,0059	0,018	0,0066	0,0002	0,0005	0,0067

TABLE II. *RESULTS OF THE LSTM OPENLOOP SUBNET TEST*

Number of LSTM Units	Number of Delays	RMSE Net 1	RMSE Net 2	RMSE Net 3	RMSE Net 4	RMSE Net 5	RMSE Net 6
5	3	0,1493	0,3373	0,4015	0,1285	0,0918	0,5018
5	6	0,1223	0,3766	0,2651	0,0986	0,0729	0,4065
10	3	0,1087	0,2451	0,2132	0,0806	0,0779	0,3441
10	6	0,1332	0,3416	0,2305	0,0787	0,0723	0,327
20	3	0,1106	0,2442	0,2095	0,0592	0,0692	0,3236
20	6	0,134	0,2909	0,2175	0,0725	0,06	0,3039

In a second test series, the input values of the true past outputs were replaced by the feedback outputs of each subnetwork. This highlighted the error accumulation generated by each subnetwork. Tables III and IV show the results with the averaged RMSE over all 3 test drives. As can be seen from the test results, the error rates for both network types increase in the partially closed loop. The NARX subnet error rate in this test series increases so dramatically that only 4 NARX subnets (Network 1, 2, 4, and 5) perform better than the LSTM subnets.

TABLE III. *RESULTS OF THE NARX PARTIAL CLOSED LOOP SUBNET TESTS*

Number of LSTM Units	Number of Delays	RMSE Net 1	RMSE Net 2	RMSE Net 3	RMSE Net 4	RMSE Net 5	RMSE Net 6
5	3	0,1493	0,3373	0,4015	0,1285	0,0918	0,5018
5	6	0,1223	0,3766	0,2651	0,0986	0,0729	0,4065
10	3	0,1087	0,2451	0,2132	0,0806	0,0779	0,3441
10	6	0,1332	0,3416	0,2305	0,0787	0,0723	0,327
20	3	0,1106	0,2442	0,2095	0,0592	0,0692	0,3236
20	6	0,134	0,2909	0,2175	0,0725	0,06	0,3039

TABLE IV. *RESULTS OF THE LSTM PARTIAL CLOSED LOOP SUBNET TESTS*

Number of LSTM Units	Number of Delays	RMSE Net 1	RMSE Net 2	RMSE Net 3	RMSE Net 4	RMSE Net 5	RMSE Net 6
5	3	1,1777	4,9163	2,3134	0,5887	0,9752	8,8424
5	6	0,5883	5,1189	2,1451	0,586	0,987	13,897
10	3	0,6478	4,2755	2,2007	0,5778	0,969	5,1603
10	6	0,6148	4,9479	2,1204	0,4728	0,9435	4,5458
20	3	0,6237	4,4588	2,1995	0,6136	0,9106	5,547
20	6	0,5667	4,747	2,1876	0,4748	0,8591	3,9582

In the final test series all coupled inputs were replaced by the linked direct and feedback outputs of the coupled individual subnets. For the combined overall model, the sub network structure, which performed best in the second test series, was selected for the respective network types. Table V shows the results with the RMSE for both network types for all 3 test drives. As can be seen from the results, the error rates of the NARX networks increase significantly, while the error rate in the LSTM subnets is almost unchanged com-

 ISBN: 978-1-61208-706-1

pared to the second test series. The error rates of the NARX networks have a greater spread compared to the error rates of the LSTM networks. This is an indication for a better generalization capability of the LSTM networks.

TABLE V. RESULTS OF THE LSTM *OVERALL* CLOSED LOOP TESTS

NARX	RMSE Net 1	RMSE Net 2	RMSE Net 3	RMSE Net 4	RMSE Net 5	RMSE Net 6
Test Drive Simulation 1	7,7141	5,7805	2,6185	9,8997	4,7859	37,936
Test Drive Simulation 2	1,5486	1,2762	0,9869	0,3264	0,1003	43,264
Test Drive Simulation 3	6,3908	1,6349	2,6705	8,4168	4,0662	37,749
LSTM	**RMSE Net 1**	**RMSE Net 2**	**RMSE Net 3**	**RMSE Net 4**	**RMSE Net 5**	**RMSE Net 6**
Test Drive Simulation 1	0,8787	4,8565	2,243	0,7314	0,8758	5,4002
Test Drive Simulation 2	0,5962	2,7291	1,73	0,3627	0,8197	3,7709
Test Drive Simulation 3	0,8667	7,2622	3,3382	0,6307	1,0455	6,5789

In summary, the test results of the overall models for the cabin air and windscreen temperature (Output Network 4 and Network 5) and the relative humidity (Output Network 6) show on average smaller error rates for the LSTM-based overall model.

VI. CONCLUSION

In the experiments, the overall LSTM-based model outperformed the overall NARX-based model for the simulation data tested. This leads to the conclusion that LSTM-based neural networks offer a promising alternative to traditional neural network modeling approaches. However, no conclusion can be drawn regarding the general suitability of the procedures. On the one hand, only a small subset of possible external climatic conditions was mapped with the generated reference data, so that no valid statement can be made about the generalizability for a broad spectrum of climatic boundary conditions. In addition, the networks were trained with "perfect" training data. Therefore, no statement can be made about the ability of the networks to what extent noisy signals or measurement inaccuracies can be compensated. For further evaluation, a wider range of test and training data must be used. To reduce the quality gap to physical reference models, more complex LSTM networks with longer input sequences, a higher number of LSTM units, and a larger number of training epochs may be required. These questions will be the subject of subsequent research based on this paper.

ACKNOWLEDGMENT

The authors acknowledge the financial support by the Federal Ministry of Education and Research of Germany in the framework of "KMU-innovativ: Informations- und Kommunikationstechnologien" within the project "Kataloggestützte interdisziplinäre Entwurfsplattform für Elektrofahrzeuge (KISEL)".

REFERENCES

[1] R. Baumgart, Reduzierung des Kraftstoffverbrauches durch Optimierung von Pkw-Klimaanlagen, Chemnitz, Germany: Dissertation TU Chemnitz, 2010.

[2] C. Haupt, Ein multiphysikalisches Simulationsmodell zur Bewertung von Antriebs- und Wärmemanagementkonzepten im Kraftfahrzeug, München, Germany: Dissertation, TU München, 2012.

[3] D. Ghebru, Modellierung und Analyse des instationären thermischen Verhaltens von Verbrennungsmotor und Gesamtfahrzeug, Frankfurt am Main: Dissertation, Karlsruher Institut für Technologie, 2013.

[4] F. Schueppel, Optimierung des Heiz- und Klimakonzepts zur Reduktion der Wärme- und Kälteleistung im Fahrzeug, Berlin, Germany: Dissertation TU Berlin, 2015.

[5] K. Schröder, S. Wagner, M. Ellinger, „Gekoppelte Simulation der Klimaanlage und Fahrgastzelle unter Berücksichtigung variierender Randbedingungen," in *PKW_Klimatisierung II- Klimakonzepte, Regelungsstrategien und Entwicklungsmethoden heute und in Zukunft*, Essen, expert verlag, 2002, pp. 210-223.

[6] H. Tummescheit, J. Eborn, K. Proessl, S. Foersterling und W. Tegethoff, „AirConditioning: Eine Modelica-Bibliothek zur dynamischen Simulation von Kältekreisläufen," in *PKW-Klimatisierung IV- Klimakonzepte, Zuheizkonzepte, Regelungsstrategien und Entwicklungsmethoden*, Essen, expert verlag, 2007, p. 196214.

[7] R. Domschke und M. Matthes, „In-the-Loop Simulation of Electronic Automatic Temperature Control Systems: HVAC Modeling," in *PKW-Klimatisierung IV- Klimakonzepte, Zuheizkonzepte, Regelungsstrategien und Entwicklungsmethoden*, Essen, expert verlag, 2006, pp. 215-231.

[8] K. Martin, R. Rieberer, S. Alber, J.-J. Robin und T. Schaefer, „Einsatz von numerischer Simulation bei der Entwicklung von Kältekreisläufen," in *PKW-Klimatisierung V-Effiziente Kältekreisläufe, Klimakonzepte für Hybridfahrzeuge und Strategien zur Komfortverbesserung*, Essen, expert verlag, 2007, pp. 77-91.

[9] S. Park, A Comprehensive Thermal Management System Model for Hybrid Electric Vehicles, Michigan, USA: Dissertation, The University of Michigan, 2011.

[10] B. Flieger, Innenraummodellierung einer Fahrzeugkabine in der Programmiersprache Modelica, RWTH Aachen: Dissertation, 2013.

[11] D. Marcos, F. J. Pino, B. Carlos und J. J. Guerra, „The development and validation of a thermal model for the cabin of a vehicle," *Applied Thermal Engineering 66*, pp. 646-656, 2014.

[12] M. Fritz, Entwicklungswerkzeuge für die Fahrzeugklimatisierung von Nutzfahrzeugen, Karlsruhe, Germany: Dissertation, Karlsruher Institut für Technologie (KIT), 2015.

[13] F. Netter, Komplexitätsadaption integrierter Gesamtfahrzeugsimulationen, Karlruhe, Germany: Dissertation, Karlsruher Institut für Technologie (KIT), 2015.

[14] D. Moller, J. Aurich, R. Tröger und C. Grünig,

„Gesamtheitliche Betrachtung des Thermomanagements in Elektrofahrzeugen - Interaktion der Klima- und Kühlsystemkomponenten im Gesamtverbund," in *19. MTZ-Fachtagung Simulation und Test 2017*, Darmstadt, Germany, 2017.

[15] S. Hochreiter und S. Jürgen, „Long Short-Term Memory," in *Neural Computation 9(8): 1735-1780*, München, Germany, 1997.

[16] T. M. Association, „FMI - Functional Mock-Up Interface," [Online]. Available: https://fmi-standard.org/. [Zugriff am 01 03 2019].

[17] G. Mustafarraj, J. Chen und G. Lowry, „Thermal behavior prediction utilizing artificial neural networks for an open office," in *Applied Mathematical Modelling 34 (2010) 3216-3230*, Uxbridge, Middlesex, United Kingdom, 2010.

[18] T. Lu und M. Viljanen, „Prediction of indoor temperature and relative humidity using neural network models: model comparison," in *Neural Comput & Applic 18: 345–357*, Espoo, Finland, 2009.

[19] P. M. Ferreira, A. E. Ruano, S. Silva und C. E.Z.E, „Neural networks based predictive control for thermal comfort and energy savings in public buildings," in *Energy and Buildings 55 238–251*, Portugal, 2012.

[20] A. E. Ruano und P. M. Ferreira, „Neural Network based HVAC Predictive Control," in *Proceedings of the 19th World Congress IFAC*, Cape Town, South Africa, 2014.

[21] T.-Y. Lee, Prediction of Car Cabin Temperature Using Artificial Neural Network, München: Master-Thesis Technische Universität München, 2007.

[22] B. C. Ng, D. I. Z. Mat, H. Jamaluddin und H. M. Kamar, „Application of adaptive neural predictive control for an automotive air conditioning system," in *Applied Thermal Engineering 73 (2014) 1242-1252*, Johor, Malaysia, 2014.

[23] B. C. Ng, D. I. Z. Mat, H. Jamaluddin und H. M. Kamar, „Dynamic modelling of an automotive variable speed air conditioning system using nonlinear autoregressive exogenous neural networks," in *Applied Thermal Engineering 73 (2014) 1253-1267*, Johor, Malaysia, 2014.

[24] TIL Suite: Software package to simulate thermal systems, TLK-Thermo GmbH, Braunschweig, March 2019.

[25] TIL AddOn Automotive: Software package to simulate thermal systems with focus on automolie applications, TLK-Thermo GmbH, Version 3.6.0 [Computer Software], Braunschweig, März 2019.

[26] Rohsenow, M. W.: Boiling, in: Rohsenow, M. W.; Hartnett, P. J; Ganic, E. N. (Editor): Handbook of Heat Transfer Fundamentals, 2. Edition, McGraw-Hill, 1985.

[27] Gnielinski, V.: Neue Gleichungen für den Wärme- und den Stoffübergang in turbulent durchströmten Rohren und Kanälen, in: Forschung im Ingenieurwesen - Engineering Research Vol. 41, Pt. 1, Springer-Verlag, 1975, pp. 8 – 16.

[28] Dittus, F. W.; Boelter, L. M. K.: Heat Transfer in Automobile Radiators of the Tubular Type, in: Publications on Engineering Vol. 2, University of California at Berkeley, 1930, pp. 443 – 461.

[29] Shah, M. M.: A New Correlation for Heat Transfer during Boiling Flow Through Pipes, in: ASHRAE Transac-tions Vol. 82, Pt. 2, American Society of Heating, Refrigerating and Air-Conditioning Engineers - ASHRAE Inc., 1976.

[30] Haaf, S.: Wärmeübertragung in Luftkühlern, in: Steimle, F. (Editor); Stephan, K. (Editor): Handbuch der Kälte-technik Vol. 6, Pt. B, Springer-Verlag, 1988.

[31] McAdams, W. H.; Woods, W. K.; Heroman, L. C.: Vaporization inside horizontal tubes-II-benzene-oil mix-tures, in: Trans. ASME Vol. 64, Pt. 3, The American Society of Mechanical Engineers, 1942, pp. 193 – 200.

[32] Swamee, P. K.; Jain, A. K.: Explicit Equations for Pipe-Flow Problems, in: Journal of the Hydraulics Division, Vol. 102, Pt. 5, ASCE - American Society of Civil Engineers, 1976, pp. 657 – 664.

[33] TIL AddOn Cabin: Software package to simulate thermal systems with focus on automobile interiors, TLK-Thermo GmbH, Version 3.6.0 [Computer Software], Braunschweig, März 2019.

 ISBN: 978-1-61208-706-1